Thermal noise response based control of tip-sample separation in AFM

Anil Gannepalli[1], Abu Sebastian[1], Jason P. Cleveland[2] and Murti V. Salapaka[1]

[1]Department of Electrical and Computer Engineering, Iowa State University, Ames, IA 50011

[2]Asylum Research, 341 Bollay Drive, Santa Barbara, California 93117-5550

Abstract—**Micro-cantilever based devices have revolutionized imaging and they are the primary tools for investigation and control of matter at the nanoscale. In certain applications like single electron spin detection, it is essential to maintain a sub-nanometer tip-sample separation for extended periods of time. The existing techniques of atomic force microscope (AFM) operation are not suited for such applications . In this paper a novel approach based on the thermal noise response of the cantilever is developed that promises to meet the aforementioned challenges. The presented technique exploits the dependence of the tip-sample separation and cantilever's resonant frequency to maintain a small tip-sample separation by regulating the effective resonant frequency. The resonant frequency is estimated from cantilever's response to the thermal noise forcing. The experiments performed in ambient room conditions have achieved tip-sample separations as small as 1.5 nm for time periods in excess of 30 min.**

I. INTRODUCTION

In the last four decades, since Richard Feynman delivered his prophetic talk [1] on the possibility of *Nanotechnology*, the scanning probe microscopes (SPM) have made the single most significant contribution towards realizing Feynman's dream. These devices, of which the micro-cantilever based atomic force microscope (AFM) [2] is the most popular, have demonstrated the feasibility of rational *control, manipulation* and *investigation* of matter at the atomic-scale.

A typical AFM, illustrated schematically in Figure 1, makes use of the forces of interaction between atoms and molecules. The AFM consists of an extremely small micro-cantilever ($50 - 200$ μm long and a few μm wide) with a sharp tip ($5 - 10$ nm diameter) that bends under the influence of interatomic interaction forces when brought very close to the sample under investigation. The deflection of the cantilever is measured by a quadrucell photodetector as a change in the reflectance angle of the incident laser. The measured deflection is used by a feedback controller to move the sample up or down via the xyz piezoelectric scanner. There are two
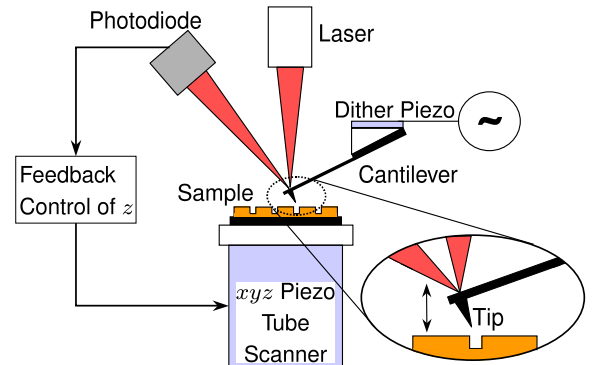

Fig. 1. A schematic of the essential components of an AFM. It consists of a tip-cantilever assembly, sampling positioning system, deflection detection system and a feedback control system.

regimes of the distance dependent tip-sample forces - long range attractive regime due to van der Waals forces and short range chemical forces that are mildly attractive and immensely repulsive. In addition there might be magnetic, electric and adhesive capillary forces in action. In the static mode of AFM operation static deflection of the cantilever caused by the tip-sample interactions is studied, where as in the dynamic mode the cantilever is forced sinusoidally and the changes in the dynamics due the tip-sample forces are monitored.

In many studies a micro-cantilever based investigation of extremely small forces evolving over large time scales is of considerable interest. One such application is the detection of single electron spin where forces in the 10^{-14} N to 10^{-16} N have to be detected [3]. In this application in order to detect the highly localized forces it is essential to maintain a tip-sample separation in the order of a few nm to a few Å. In addition such separations have to be maintained with good separation stability for extended periods of time. This is a requirement is imposed either by the time scales of the dynamic process being studied or the need to average to achieve the necessary sensitivity or both. Another application is the study of biomolecular interactions

whose dynamics have timescales of microseconds to milliseconds. The tremendous scope of the AFM to study the biomolecular dynamics has been amply demonstrated [4], [5], [6], [7]. However, most of these studies are invasive wherein the tip is in contact with the specimen. In such studies the effect of the tip-sample contact on the dynamics is difficult to characterize. For applications like spin detection the cantilever tip is too obtrusive if it encounters the repulsive region of the tip-sample potential. This necessitates non-contact operation with extremely small rms tip deflections. A primary hurdle for non-contact operation in static mode is the $1/f$-noise and drift of the system that becomes particularly detrimental over long time periods. These drift effects are due to uncertain factors like changes in the deflection detector [8], [9], thermal bending [10], [11] and creep in the piezo based positioner. Low temperatures can alleviate problems associated with drift but such conditions are not always conducive to the study. Furthermore, static mode methods cannot differentiate between attractive and repulsive interactions thereby making it unsuitable for maintaining the tip in the attractive regime. Classic dynamic methods overcome some of the above issues and can be used in non-contact operation. However, they are associated with large amplitudes that are un-acceptable to applications such as spin detection. Small amplitudes in frequency modulation (FM-AFM) scheme are proposed [12] for optimal resolution, wherein the frequency shifts are larger and are solely due to the highly local short range interactions. Consequently small amplitudes are favorable for achieving true atomic resolution and considerable success has been demonstrated [13], [14]. However this necessitates low temperature operation to suppress thermal vibrations. One method that has not received much attention since its mention [15], is the use of thermal vibrations of the cantilever in FM-AFM. Such a technique has the advantages of dynamic mode and is an attractive approach to study small bandwidth dynamics.

In this study we develop the FM technique based on the thermal noise response of the cantilever that promises to meet the demands of maintaining sub-nanometer separations over large time periods. It also enables the detection of forces in the order of a few pN. In effect we demonstrate static non-contact atomic force microscopy.

II. THEORY AND MODEL

The cantilever is modeled as a single spring-mass-damper system (see Figure 2) as described by

$$m\ddot{p}(t) + c\dot{p}(t) + kp(t) = \eta(t) + F(t), \qquad (1)$$

where $p(t)$ is the cantilever deflection, m is the mass of the cantilever, c is the damping constant, k is the spring constant and $\eta(t)$ is the Langevin thermal noise forcing term and $F(t)$ describes other external forces acting on the cantilever. As alluded above, the cantilever is very small and has perceptible response to the thermal noise forcing. The power spectral density of deflection of a cantilever in thermal equilibrium $\frac{1}{2}k_BT = \frac{1}{2}k\langle p^2 \rangle$ in the absence of external forcing ($F(t) = 0$) is given by [16]

$$S_{pp}(\omega) = \frac{4\omega_0 k_B T}{Qm} \frac{1}{(\omega_0^2 - \omega^2)^2 + (\frac{\omega_0 \omega}{Q})^2}, \qquad (2)$$

where k_B is Boltzmann's constant and T is the temperature. The resonant frequency is given by

$$\omega_R = \omega_0 \sqrt{1 - \frac{1}{4Q^2}}, \qquad (3)$$

where ω_0 ($= \sqrt{k_0/m}$) is the undamped resonant frequency and Q ($= \frac{\omega_0 m}{c}$) is the quality factor of the cantilever.
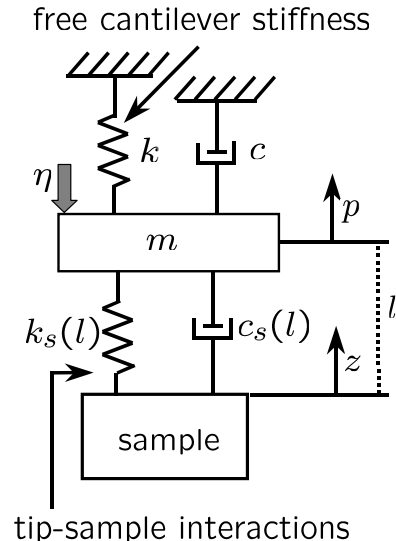

Fig. 2. The cantilever is modeled by the spring-mass-damper system. The effect of the tip-sample interactions is modeled by a nonlinear spring whose stiffness depends on the tip-sample separation.

When the tip interacts with the sample, the tip-sample forces ($F(t) = F_s(t)$) alter the cantilever dynamics. The tip-sample forces can be modeled as a spring-damper system (see Figure 2) by separating the conservative and dissipative interactions as

$$F_s(l(t), \dot{l}(t)) = -k_s(l)l(t) - c_s(l)\dot{l}(t), \qquad (4)$$

where k_s $\left(= -\frac{\partial F_s}{\partial l}\big|_l\right)$ is the force gradient and c_s $\left(= -\frac{\partial F_s}{\partial \dot{l}}\big|_l\right)$ accounts for the dissipation. In such a scenario the changes in the cantilever dynamics can

be analyzed by linearizing about an equilibrium state (denoted by *) as below

$$m\ddot{\delta p}(t) + c\dot{\delta p}(t) + k\delta p(t) = \eta(t) - c_s^*\dot{\delta l}(t) - k_s^*\delta l(t) \quad (5)$$

where $\delta z(t) = z(t) - z^*$, $\delta l(t) = l(t) - l^*$, $\delta p(t) = p(t) - p^*$ are the deviation variables. Observing $\delta l = \delta p - \delta z$ from Figure 2 it follows that

$$m\ddot{\delta p}(t) + c_{eff}\dot{\delta p}(t) + k_{eff}\delta p(t) = \eta(t) + c_s^*\dot{\delta z}(t) + k_s^*\delta z(t) \quad (6)$$

where k_{eff} $(= k + k_s^*)$ is the effective spring constant and c_{eff} $(= c + c_s^*)$ is the effective damping constant. Therefore, the tip-sample interactions have the effect of altering the effective spring and damping constant thereby changing the resonant frequency of the cantilever. For small tip-sample forces, large Q and negligible near surface damping, the resonant frequency shift $\Delta\omega_R$ can be approximated by the relation

$$\Delta\omega_R \approx \omega_R \frac{k_s^*}{2k}. \quad (7)$$

The effective resonant frequency $\omega_{R,eff}$ $(= \omega_R + \Delta\omega_R)$ decreases (increases) when the tip-sample interaction force is attractive (repulsive). Thus, by observing the effective resonant frequency the attractive and repulsive regimes of the interaction potential can be differentiated. The information about $\omega_{R,eff}$ is available in the power spectral density of the thermal noise response as a shift in the peak position of the power spectrum. In this work this fact is utilized to control the tip-sample separation by regulating the effective resonant frequency. One essential requirement is that the cantilever spring constant be large enough to avoid any jump-to-contact instabilities in the region of operation $(k + k_s^* > 0$ for all $l^*)$.

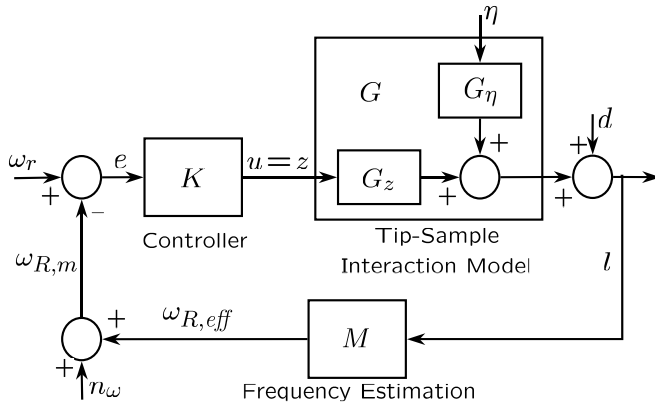## III. CONTROL SCHEME: SYSTEMS VIEW

Fig. 3. A schematic block diagram of the closed loop

Maintaining a constant tip-sample separation translates into a problem of regulating the effective resonant frequency of the cantilever at a desired value

as illustrated in the proposed control architecture in Figure 3. For a high Q cantilever, its thermal noise response as observed in the deflection signal is assumed to be a single sinusoid in white noise. The frequency of this sinusoid, corresponding to the effective resonant frequency of the cantilever, is estimated by Pisarenko harmonic decomposition (PHD) [17].

The block G refers to the cantilever interacting with the sample and consists of the transfer functions $G_z(s)$ and $G_\eta(s)$. $G_z(s)$ accounts for the dependence of the tip-sample separation l on the sample position z and $G_\eta(s)$ represents the effect of η on l. Rewriting Eq. (5) in terms of δl and δz and applying Laplace transform yields the following expression for G_z and G_η

$$\delta l(s) = G_z(s)\delta z(s) + G_\eta(s)\eta(s), \quad (8a)$$

$$G_z(s) = \frac{-(ms^2 + cs + k)}{ms^2 + c_{eff}s + k_{eff}}, \quad (8b)$$

$$G_\eta(s) = \frac{1}{ms^2 + c_{eff}s + k_{eff}}. \quad (8c)$$

$M(s)$ represents the dependence of $\omega_{R,eff}$ on l. For small variations in l, $M(s)$ can be approximated by a simple gain as

$$M(s) = m^* = \left.\frac{\partial\omega_{R,eff}}{\partial l}\right|_{l^*}. \quad (9)$$

$K(s)$ is the feedback control law actuating the z-motion of the sample, via the control output u, in an effort to maintain the measured resonant frequency ω_m at the desired value ω_r. n_ω represents the noise in the frequency estimation. The effect of the drift processes is modeled as a disturbance d in the sample position.

In order to maintain a constant l the control scheme should be capable of compensating for the disturbances d. Additionally, for good resolution the effect of the frequency noise n_ω on l should be minimal. These dependencies are expressed as $S = \frac{1}{1+G_zKM}$ and $T = \frac{G_zKM}{1+G_zKM}$ respectively. S is the sensitivity transfer function that needs to be small in the frequency band where disturbances are present for good disturbance rejection. T is the complementary sensitivity function that needs to be small so as to minimize the effects of noise. Therefore, S is a measure of disturbance rejection and T is a measure of resolution. Since,

$$S(\omega) + T(\omega) = 1, \quad (10)$$

T has to be large when S is small and vice-versa. The closed loop bandwidth B is defined as the frequency at which $|S(\omega)|$ crosses -3 dB from below. Therefore, the controller K should be designed such that

$$|S(\omega)| < 1, \quad \omega < \omega_B \quad (11a)$$

$$|T(\omega)| < 1, \quad \omega > \omega_T(\approx \omega_B) \quad (11b)$$

where $\omega_B = 2\pi B$ is the upper bound on the bandwidth of d. Hence, these transfer functions capture the classic trade off between bandwidth and resolution.

Any other disturbance in the tip-sample forces that has a bandwidth greater than the closed loop bandwidth of the system B, will not be acted upon by the controller and will potentially show up as a variation in the cantilever's resonance. This is the principle behind the use of this technique to monitor variations in tip-sample interaction forces. Therefore, for imaging the controller should be designed such that the closed loop bandwidth is intermediate to that of the disturbance and the imaging signal. This work is in progress.

IV. RESOLUTION AND BANDWIDTH

The vertical resolution, defined as the smallest change in tip-sample separation that can be resolved, is limited by the noise in the tip-sample separation. The achievable vertical resolution is crucial to the success of the proposed method. It is, therefore, important to identify all the possible sources of noise which will limit the resolution. The two major sources of vertical noise are (1) fluctuations in sample position σ_z^2 and (2) thermal fluctuations of the cantilever $\sigma_{p_{th}}^2$.

The noise in sample position is a consequence of the frequency noise n_ω being fed back in the control scheme. This frequency noise has three sources (1) thermal fluctuations of the cantilever, (2) noise in the deflection sensor and (3) the noise in the frequency estimation method. The transfer function between δz and n_ω from Figure 3 is

$$\delta z(s) = -\frac{K(s)}{1 + G_z(s)M(s)K(s)}n_\omega(s). \quad (12)$$

Eq. (8a) can therefore be rewritten as

$$\delta l(s) = -\frac{G_z(s)K(s)}{1 + G_z(s)M(s)K(s)}n_\omega(s) + G_\eta(s)\eta(s). \quad (13)$$

Recognizing $\frac{G_z K}{1 + G_z MK} = \frac{1}{m^*}T$, the power spectral density of $\delta l(t)$, when $n_\omega(t)$ and $\eta(t)$ are statistically independent, is given by

$$S_{ll}(\omega) = \frac{1}{m^{*2}}\left|T(\omega)\right|^2 S_{\omega\omega}(\omega) + \left|G_\eta(\omega)\right|^2 S_{\eta\eta}(\omega). \quad (14)$$

where $S_{\omega\omega}(\omega)$ and $S_{\eta\eta}(\omega)$ are the power spectral densities of $n_\omega(t)$ and $\eta(t)$ respectively.

Observing $\frac{1}{2\pi}\int_0^\infty \left|G_\eta(\omega)\right|^2 S_{\eta\eta}(\omega)d\omega = \sigma_{p_{th}}^2$ and substituting $M(\omega) = m^*$ the expression for vertical noise, when the frequency estimates have a noise density ρ_{FE}, reduces to

$$\sigma_l^2 = \frac{\rho_{FE}}{m^{*2}}B + \sigma_{p_{th}}^2 \quad (15)$$

where $\omega_B = 2\pi B$. This clearly illustrates the trade off between between bandwidth and resolution where a small B will enhance the sensitivity and resolution as noted in the previous section.

V. EXPERIMENTAL RESULTS

The thermal noise based non-contact mode operation was demonstrated in a variety of experiments few of which are discussed below. The experiments are performed on a Digital Instruments Multimode AFM in ambient environment. The signal processing for frequency estimation and the controller are implemented on a TMS320C44 digital processing platform. Silicon cantilevers with a nominal $Q = 450, k = 1$ N/m and $\omega_0 = 350$ kHz were used. The sample surface was freshly cleaved HOPG. The frequency estimates were available at a bandwidth $B_{FE} = 265$ Hz with a noise density $\rho_{FE} \approx 600$ Hz^2/Hz. The observed noise in deflection sensor was $\rho_{DS} = 10^{-6}$ Hz^2/Hz. For these experimental parameters the total theoretical lower limit for the frequency noise calculated from Eqs. (**??**) and (**??**) is about 400 Hz^2/Hz. The observed frequency noise is significantly higher due to the algorithmic deficiencies in implementation that can be significantly improved in future.
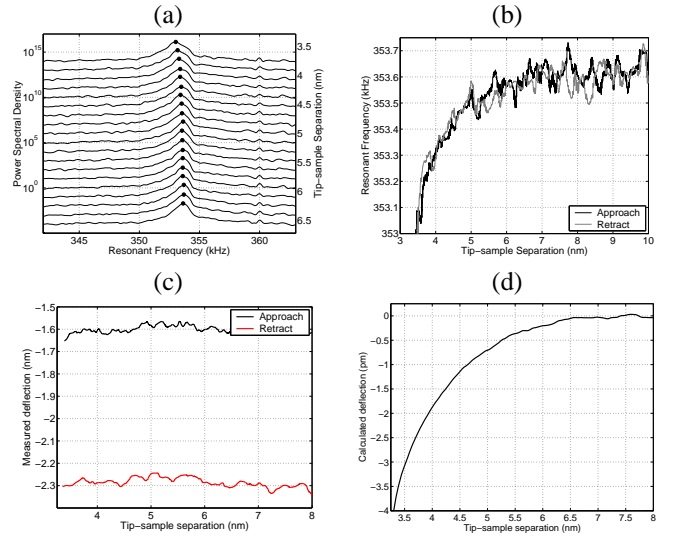

Fig. 4. (a) The effect of tip-sample forces on the cantilever's thermal noise response. The variation in (b) estimated resonant frequency (c) cantilever deflection with tip-sample separation. The calculated deflection $p_{calc} = \frac{2}{\omega_0}\int \Delta\omega dl$ (see Eqn.(7)) for the frequency changes observed in (b).

Figure 4(a) shows the observed changes in the thermal noise response of the cantilever as it interacts with the sample. In Figure 4(b) the variation in the estimated cantilever's resonant frequency as a function of tip-sample separation during approach and retraction is shown. It

is seen that the resonant frequency decreases due to the long range attractive tip-sample interactions. The strength of these attractive forces increases with a decreasing tip-sample separation. However, a similar effect is not observed in the deflection as seen in Figure 4(c). This is because the maximum observable deflection (see Figure 4(c)) estimated to be approximately 4 pm is much smaller than the deflection sensitivity of the instrument at low bandwidths.
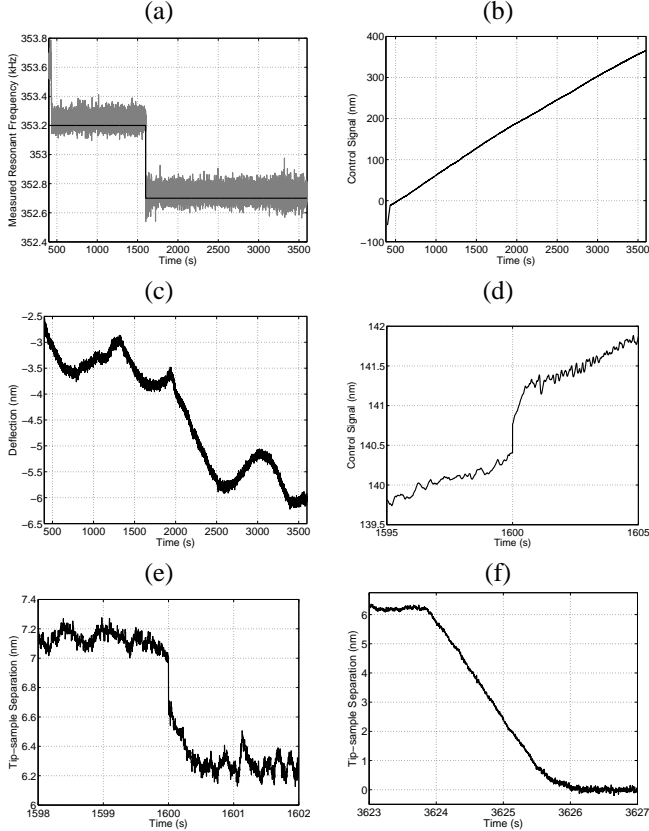

Fig. 5. Time history of (a) estimated frequency (b) control effort and (c) deflection while tracking a step change in reference frequency shown in (a). The step response in (d) control effort and (e) tip-sample separation. (f) Tip-sample separation just before tip-sample contact.

The following experiment demonstrates the feasibility of the proposed method to control the tip-sample separation. In this experiment a step change is given to the reference frequency. The cantilever resonant frequency estimates, control signal and deflections are shown in Figure 5(a), (b) and (c) respectively. In the initial stages of the control, the tip is not interacting with the sample and the measured resonance is 353.6 kHz (see Figure 5(a)), which is the free resonant frequency of the cantilever. The controller, therefore, acts to move the sample towards the tip as seen in Figure 5(b). Once the desired tip-sample separation is achieved, indicated by the resonant frequency being close to the reference,

the control action counteracts the drift in the instrument. At approximately 1600 s into the experiment the step change in the reference is introduced and the controller is able to track this change. As the reference is reduced, implying a smaller desired tip-sample separation, the controller moves the sample towards the tip and is seen as a small "spike" in Figure 5(d) at 1600 s. This control action results in a reduction in tip-sample separation as seen in Figure 5(e). The new reference is reached in less than 1 s. As reasoned earlier, the variations in deflection in Figure 5(c) can be attributed to the drift in the deflection sensor as the tip-sample forces are too small to induce any perceivable change in the deflection. This drift compensation indicates that the closed-loop bandwidth of 1 Hz is larger than the bandwidth of the drift processes in the system. Figure 5(f) shows that the tip-sample distance of about 6.3 nm is maintained for over 30 mins until the experiment was terminated.
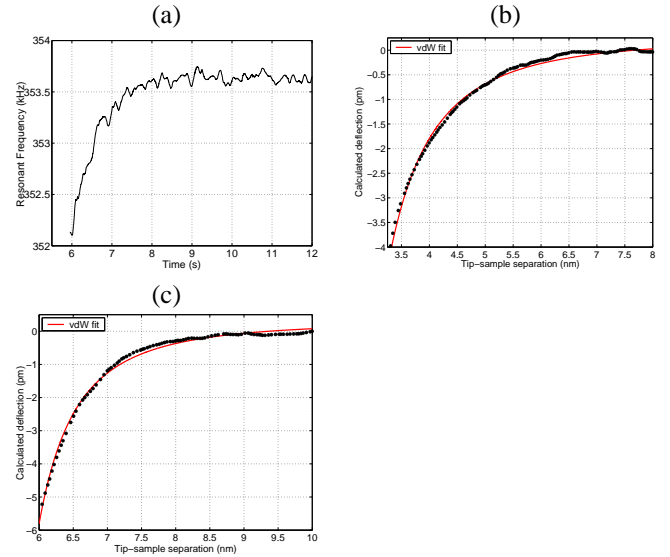

Fig. 6. (a) Updated dependence of the resonant frequency the tip-sample separation. (b) Cantilever deflection as shown in Figure 4(c) as dots with a van der Waals type force $\left(F_{vdW} = \frac{A}{(l_0+l)^2(l+l_0+2R)^2} \right)$ fit. A value of 10 nm is used for the tip radius R and the thickness of the surface contamination is estimated to be $l_0 \approx 1.6$ nm. (c) A similar plot for the frequency changes in 6(a). The surface layer thickness is estimated at $l_0 \approx 4.9$ nm yielding a true tip-sample separation of about 1.5 nm throughout the experiment.

It is interesting to note that a separation of 6.3 nm doesn't agree with the corresponding separation for a resonant frequency of 352.7 kHz in Figure 4(a). This discrepancy can be attributed to the changes in the tip-sample interactions due to the adsorption of moisture and other adsorbates in ambient air on the sample surface during the long time duration (> 1 hour) of the experiment. Therefore, a more accurate description of tip-sample interactions will be provided by the approach

part of a force curve performed immediately after the experiment. Figure 6 shows the current state of the tip-sample interactions and it can be seen that a resonant frequency of 352.7 kHz does indeed correspond to a tip-sample separation of about 6.3 nm. Therefore, it is more accurate to refer to the surface contamination as the sample and the true tip-sample separation can be estimated fitting a van der Waals type force to the observed force dependence on the tip-sample separation. Figure 6 shows the cantilever deflections calculated from the observed frequency changes in Figs. 4(a) and 6(a). The fits yield a contamination layer thickness of 1.6 nm the beginning of the experiment which has increased in thickness to 4.9 nm by the end. This gives a separation of about 1.5 nm between the tip and the surface contamination throughout the experiment. In addition, a change of 0.7 nm in the tip-sample separation (see Figure 5(e)) induced by a step change in the reference correlates well with the change required for a reduction in the resonance from 353.2 kHz to 352.7 kHz (see Figure 6(a)).

VI. CONCLUSIONS

A novel static non-contact mode of operation of AFM based on the thermal noise response of the cantilever has been demonstrated. In this approach cantilever's thermal noise response is used to estimate the changes in its resonant frequency that is fed back for maintaining the tip-sample separation. The model uncertainty associated with the nonlinear tip-sample interactions and the noisy frequency estimates necessitate the use of slow controllers. This feature enables this technique to monitor and observe signals with a frequency content intermediate to the closed loop bandwidth and the cantilever resonant frequency. The experiments performed in ambient room conditions have achieved tip-sample separations as small as 1.5 nm for periods extending over 30 min. A better design of instrumentation and controlled experimental conditions promise improved performance of this technology.

VII. ACKNOWLEDGEMENTS

REFERENCES

[1] R. Feynman, "There's Plenty of Room at the Bottom," 1959.

[2] G. Binning, C. F. Quate, and C. Gerber, "Atomic force microscope," *Phys. Rev. Lett.*, vol. 56, pp. 930, 1986.

[3] K. Holczer, "Development of a single electron spin microscope," DARPA, MOSAIC Proposal, 2001.

[4] R. Eckert, S. Jeney, and J. K. H. Hörber, "Understanding intercellular interactions and cell adhesion: Lessons from studies on protein-metal interactions," *Cell Biol. Int.*, vol. 21, no. 11, pp. 707, November 1997.

[5] A. Razatos, Y-L. Ong, M. M. Sharma, and G. Georgiou, "Molecular determinants of bacterial adhesion monitored by atomic force microscopy," *Proc. Natl. Acad. Sci.*, vol. 95, pp. 11059, September 1998.

[6] M. Stolz, D. Stoffler, U. Aebi, and C. Goldsbury, "Monitoring biomolecular interactions by time-lapse atomic force microscopy," *J. Struct. Biology*, vol. 131, pp. 171, 2000.

[7] M. Mondon, S. Berger, and C. Ziegler, "Scanning-force techniques to monitor time-dependent changes in topography and adhesion force of proteins on surfaces," *Anal. Bioanal. Chem.*, vol. 375, pp. 849, 2003.

[8] G. Meyer and N. M. Amer, "Novel optical approach to atomic force microscopy [Appl. Phys. Lett. 53, 1045 (1988)]," *Appl. Phys. Lett.*, vol. 53, no. 24, pp. 2400, 1988.

[9] D. Rugar, H. J. Mamin, R. Erlandsson, J. E. Stern, and B. D. Terris, "Force microscope using a fiber-optic displacement sensor," *Rev. Sci. Instrum.*, vol. 59, no. 11, pp. 2337, November 1988.

[10] M. Radmacher, J. P. Cleveland, and P. K. Hansma, "Improvement of thermally induced bending of cantilevers used for afm," *Scanning*, vol. 17, no. 2, pp. 117, 1995.

[11] M. B. Viani, T. E. Schäffer, and A. Chand, "Small cantilevers for force spectroscopy of single molecules," *J. App. Phys.*, vol. 86, no. 14, pp. 2258, August 1999.

[12] F. J. Giessibl, H. Bielefeldt, S. Hembacher, and J. Mannhart, "Calculation of the optimal imaging parameters for frequency modulation atomic force microscopy," *Appl. Surf. Sci.*, vol. 140, pp. 352, 1999.

[13] F. J. Giessibl, S. Hembacher, H. Bielefeldt, and J. Mannhart, "Subatomic features on the silicon (111)-(7×7) surface observed by atomic force microscopy," *Science*, vol. 289, pp. 422, July 2000.

[14] F. J. Giessibl, H. Bielefeldt, S. Hembacher, and J. Mannhart, "Imaging of atomic orbitals with the atomic force microscope - Experiments and simulations," *Ann. Phys. (Leipzig)*, vol. 10, pp. 887, 2001.

[15] Giessibl F. J., "Atomic force microscopy in ultrahigh vacuum," *Jpn. J. Appl. Phys. Part I*, vol. 33, no. 6B, pp. 3726, 1994.

[16] M. V. Salapaka, H. S. Bergh, J. Lai, A. Majumdar, and E. McFarland, "Multi-mode noise analysis of cantilevers for scanning probe microscopy," *J. App. Phys.*, vol. 81, no. 6, pp. 2480, March 1997.

[17] V. F. Pisarenko, "The retrieval of harmonics from a covariance function," *Geophysics. J. Roy. Astron. Soc.*, vol. 33, pp. 347, 1973.

[18] U. Dürig, O. Züger, and A. Stalder, "Interaction force detection in scanning probe microscopy: Methods and applications," *J. App. Phys.*, vol. 72, no. 5, pp. 1778, September 1992.

[19] F. J. Giessibl, *Noncontact Atomic Force Microscopy*, chapter Principle of NC-AFM, p. 11, NanoScience and Technology. Springer, Berlin, 2002.

[20] B. G. Quinn and E. J. Hannan, *The Estimation and Tracking of Frequency*, Cambridge Series in Statistical and Probabilistic Mathematics. Cambridge University Press, Cambridge, UK, 2001.

[21] H. C. So, "Acomparative study of three recursive least-squares algorithms for single-tone frequency tracking," *Signal Processing*, vol. 83, pp. 2059, 2003.